Data-aided Carrier Frequency Offset Estimation for Orthogonal Frequency Division Multiplexing Communication Systems

Bo Xia
Department of Automation
Shanghai Jiao Tong University
Shanghai, China
boxia.sjtu@qq.com

*Yiyin Wang
Department of Automation
Shanghai Jiao Tong University
Shanghai, China
yiyinwang@sjtu.edu.cn

Genke Yang
Department of Automation
Shanghai Jiao Tong University
Shanghai, China
gkyang@sjtu.edu.cn

***Abstract*—This paper is to investigate the carrier frequency offset estimation for an orthogonal frequency division multiplexing (OFDM) communication system. Originating from the Fourier transform, OFDM uses the modulation of the amplitude and phase of subcarriers for communications. We propose a new approach that use the bit-error rate (BER) and the minimum square error (MSE) of the pilot as merits to achieve the carrier frequency offset (CFO) estimation of OFDM. The proposed method achieves lower root mean squared error (RMSE) of CFO and BER on OFDM compared with conventional methods.**

***Keywords*—Orthogonal frequency division multiplexing (OFDM), minimum square error (MSE), bit-error rate (BER), carrier frequency offset (CFO)**

I. Introduction

Orthogonal frequency division multiplexing (OFDM) is a wireless communication technology. Multiple subcarriers with the same bandwidth are orthogonal multiplexed to achieve the maximum communication rate [1]. The phase and amplitude of subcarriers can be modulated to carry information [5]. The modulated subcarriers are orthogonal and do not interfere with each other during transmission. The discrete Fourier transform (DFT) is used to realize the digital implementation of an OFDM system. Due to the clock differences between transmitters and receivers, the carrier frequency offset (CFO) destroys the orthogonality among subcarriers, and the resulting intercarrier interference degrades the BER performance severely [14]. Thus, accurately estimating the CFO to relieve its effects, is very important for restoring the symbols correctly and realizing high quality communications in OFDM systems [15].

Methods of CFO estimation can be divided into data-aided schemes [2][7] and non-data-aided (blind) ones for OFDM systems [8]-[13], [4] and [6]. An one-dimensional search-based CFO estimation is proposed in [2] using the minimum square error (MSE) of the pilot as a metric for DFT-precoded multiple-input multiple-output (MIMO) OFDM underwater acoustic communications. In [7], a training method based on the transmission of an OFDM symbol with identical halves is proposed to estimate CFO. In [4], a blind estimation method is proposed and a maximum likelihood CFO estimator is established based on two continuous and identical received blocks, where the candidate CFO is limited to less than half of the subcarrier interval. In [1], the authors investigate identifiability of non-data-aided schemes for CFO estimation based on null subcarriers. They show that the conventional approaches might suffer from channel zeros on the FFT grid and propose a new approach where the null subcarriers are placed with distinct spacings.

The method in [2] obtaining the MSE of the pilot to conduct CFO estimation has a good effect under ideal circumstances without the effect of multipath and noise. However, we find that there are several local minimums with similar values of the square error of the pilot. With the complexity of multipath and noise, these minimum points are easily confused, Thus sometimes the correct minimum value cannot be obtained by using this method. The correct CFO cannot be estimated. Sequentially, we observe that the interval where the BER of the pilot is close to zero contains the correct MSE of the pilot. Thus in this paper, we propose firstly we can use the BER of the pilot to determine the interval which contains the correct CFO value leading to the MSE of the pilot. Then, we use the MSE of the pilot to obtain the CFO estimate. The improved algorithm can achieve good performance under the multipath effect and Gaussian white noise on CFO estimation. We successfully estimate the CFO of OFDM system through simulation, the error of the estimated CFO is lower, and the signal recovered after channel equalization and CFO compensation also has a lower BER than the one in [2].

Notation: $(.)^*$, $(.)^{\mathcal{T}}$ and $(.)^{\mathcal{H}}$ stands for conjugate, transpose and Hermitian transpose respectively. $\mathbf{a} * \mathbf{b}$ denotes the convolution operation between $\mathbf{a}$ and $\mathbf{b}$. $\mathbf{A}^\dagger$ denotes the pseudo inverse of the matrix $\mathbf{A}$. Matrix $\mathbf{I}_N$ denotes a $N \times N$ identity matrix and $\mathbf{0}_{1\times N}$ stands for the $1 \times N$ all-zeros vector. Moreover, $X_{i,j}$ denotes the i-th row of the j-th column of $\mathbf{X}$. Finally, $\mathbf{S}^P$ and $\mathbf{S}^D$ denotes the pilot part and the data

Part of this work was supported by the National Nature Science Foundation of China under the grants 61633017 and 61773264, and the United Fund of Department of Equipment Development and Ministry of Education of China under the grant 6141A02033317.

part of the signal $\mathbf{S}$, respectively.

II. System Model

We consider an OFDM block transmission with a cyclic prefix (CP) to avoid interblock interference (IBI). An OFDM block consists of P pilot symbols and D data symbols, thus the block length $K = P + D$. The chirps with indices from the set $\mathcal{P}$ ($\mathcal{P} = \{I_1, I_2, ..., I_P\}$) are reserved for the pilot symbols and the chirps with indices from the set $\mathcal{D}$ ($\mathcal{D} = \{J_1, J_2, ..., J_D\}$) are taken by the data symbols. The set $\mathcal{D}$ and the set $\mathcal{P}$ constitute the set $\mathcal{K} = \{0, 1, 2, ..., K-1\}$. The pilot symbols are used for both the channel estimation and the CFO estimation on the receiver side. The symbol vector is represented as $\mathbf{x} = [S_0, S_1, ..., S_k, ..., S_{K-1}]^T$, in which the pilot symbols are marked as $\{S_{I_1}, S_{I_2}, ..., S_{I_p}, ...S_{I_P}\}$ and the data symbols are marked as $\{S_{J_1}, S_{J_2}, ..., S_{J_d}, ...S_{J_D}\}$. After modulating $\mathbf{S}$ with the IDFT matrix $\mathbf{F}^{\mathcal{H}}$, we obtain a time domain signal

$$\mathbf{s} = \mathbf{F}^{\mathcal{H}}\mathbf{S} \tag{1}$$

where $\mathbf{s} = [s_0, s_1, ..., s_k, ..., s_{K-1}]^T$. In order to eliminate the intersymbol interference caused by the multipath effect, the CP is inserted by the matrix $\mathbf{T}_{\text{cp}} = \left[\mathbf{I}^T_{\overline{L}\times K}\ \mathbf{I}^T_K\right]^T$, where $\overline{L}$ is the length of the CP. It is longer than the maximum channel delay L, and $\mathbf{I}_{\overline{L}\times K}$ consists of the last $\overline{L}$ rows of $\mathbf{I}_K$ [1]. After the insertion of the CP, we obtain the transmitted signal:

$$\mathbf{u} = \mathbf{T}_{\text{cp}}\mathbf{s} = \mathbf{T}_{\text{cp}}\mathbf{F}^{\mathcal{H}}\mathbf{S} \tag{2}$$

where the transmitted signal $\mathbf{u} = [u_0, u_1, ..., u_n, ..., u_{N-1}]^T$ with the length $N = \overline{L} + K$.

The signal suffers from the multipath effect and CFO after propogating through the channel. The n-th component of the recieved signal is represented as

$$\bar{r}_n = e^{j\omega_o n}\sum_{l=0}^{L} h(l)u_{n-l} + w_n \tag{3}$$

where $\{h(l)\}_{l=0}^{L}$ is the order-L multipath channel with a total number of $L+1$ paths. ω_o is the CFO and w_n is the additive noise with a power of σ_w^2. The matrix form of (3) can be expressed as

$$\bar{\mathbf{r}} = \mathbf{D}_N(\omega_0)(\mathbf{H}_0\mathbf{u} + \mathbf{H}_1\bar{\mathbf{u}}) + \mathbf{w} \tag{4}$$

where $\bar{\mathbf{r}} = [\bar{r}_0, \bar{r}_1, ..., \bar{r}_n, ..., \bar{r}_{N-1}]^T$, and $\mathbf{D}_N(\omega_0) = diag[1, \exp(j\omega_0), \ldots, \exp(j(N-1)\omega_0)]^T$.The channel matrix $\mathbf{H}_0$ is a $N \times N$ lower triangular Toeplitz, and $\mathbf{H}_1$ is a $N \times N$ upper triangular Toeplitz. $\mathbf{H}_0$'s first column is $[h(0), h(1), ..., h(L), 0, ..., 0]^T$ and $\mathbf{H}_1$'s first row is $[0, ..., 0, h(L), h(L-1), ..., h(1)]$ [4]. $\bar{\mathbf{u}}$ is the symbol from the previous block. Furthermore, $\mathbf{w} = [w_0, w_1, ..., w_{N-1}]^T$ is the additive white Gaussian noise (AWGN) vector.

The CP is removed at the receiver by deleting the first $\overline{L}$ elements of $\bar{\mathbf{r}}$ in (7). This is accomplished through the CP removing matrix $\mathbf{R}_{\text{cp}} = \left[\mathbf{0}_{K\times\overline{L}}\ \mathbf{I}_K\right]$ that yields $\mathbf{r} = \mathbf{R}_{\text{cp}}\bar{\mathbf{r}}$. $\mathbf{R}_{\text{cp}}\mathbf{H}_1 = \mathbf{0}_{N\times P}$ and we confirm that $\mathbf{R}_{\text{cp}}\mathbf{D}_N(\omega_o) = e^{j\omega_o\overline{L}}\mathbf{D}_K(\omega_o)\mathbf{R}_{\text{cp}}$ [1]. Using (4) and the expression for $\mathbf{u}$ from (2), defining $\mathbf{H} = \mathbf{R}_{\text{cp}}\mathbf{H}_0\mathbf{T}_{\text{cp}}$ and $\mathbf{v} = \mathbf{R}_{\text{cp}}\mathbf{w}$, we obtain the following input-output relationship after the CP removal

$$\mathbf{r} = e^{j\omega_o\overline{L}}\mathbf{D}_K(\omega_o)\mathbf{H}\mathbf{F}^{\mathcal{H}}\mathbf{S} + \mathbf{v} \tag{5}$$

It is easily verified that $\mathbf{H}$ is a circulant matrix with $[\mathbf{H}]_{k,l} = h((k-l) \bmod N)$. For wireless communications, the CFO estimation is a typical issue, and a proper estimation and compensation is necessary for achieving a good system performance.

III. The proposed CFO estimating method

In this section, we investigate CFO estimation. The algorithm flow is shown in Fig. 1, which consists of the CFO estimation and compensation unit, the channel estimation and equalization unit, and the DnFT demodulation unit. Through these operations, we can ultimately obtain the resumed signal $\hat{\mathbf{S}}$, which contains the original information. Since both the channel and the CFO are unknown, we estimate them alternatively. Firstly, we ignore the channel to estimate the initial CFO as $\hat{\omega}_0^{(0)}$, and we utilize $\hat{\omega}_0^{(0)}$ to conduct the tentative CFO compensation. Then we estimate the channel as $\hat{\mathbf{H}}^{(0)}$ based on the tentative CFO compensation. In turn, we proceed the tentative channel equalization with $\hat{\mathbf{H}}^{(0)}$, based on which we obtain a more accurate CFO estimation $\hat{\omega}^{(1)}$. Then we repeat the above steps for M (M is about 5) times to obtain the precise CFO estimation $\hat{\omega}_0$ and channel estimation $\hat{\mathbf{H}}$. Afterwards, we conduct the CFO compensation and the channel equalization, respectively, with $\hat{\omega}_0$ and $\hat{\mathbf{H}}$. Ultimately, the DFT demodulation is proceeded to obtain the resumed signal $\hat{\mathbf{S}}$.

A. Channel Estimation

Assume that we already have tentatively compensate CFO with $\hat{\omega}_0^{(i)}$, As the iterations progress, $\hat{\omega}_0^{(i)}$ becomes more precise. Thus, we just regard $e^{-j\hat{\omega}_0^{(i)}\overline{L}}\mathbf{D}_K\left(-\hat{\omega}_0^{(i)}\right)$ approximately eliminate the CFO, which can be indicated as

$$\mathbf{r}_h = e^{-j\hat{\omega}_0^{(i)}\overline{L}}\mathbf{D}_K\left(-\hat{\omega}_0^{(i)}\right)\mathbf{r} \approx \mathbf{H}\mathbf{F}^{\mathcal{H}}\mathbf{S} + \mathbf{v}_h \tag{6}$$

where $\mathbf{r}_h$ is prepared for further channel estimation, and $\mathbf{v}_h = e^{-j\hat{\omega}_0^{(i)}\overline{L}}\mathbf{D}_K\left(-\hat{\omega}_0^{(i)}\right)\mathbf{v}$. Furthermore,

$$\mathbf{r}_h = \mathbf{H}\mathbf{s} + \mathbf{v}_h = \mathbf{h} * \mathbf{s} + \mathbf{v}_h \tag{7}$$

We apply DFT transform on both sides of (7) to express it in the frequency domain as

$$\mathbf{R}_h = \mathbf{S}_d\tilde{\mathbf{F}}\mathbf{h} + \mathbf{V}_h \tag{8}$$

where $\mathbf{R}_h = \mathbf{F}\mathbf{r}_h$, $\mathbf{S}_d = diag\{\mathbf{S}\}$, and $\tilde{\mathbf{F}}$ consists of the first $L+1$ columns of $\mathbf{F}$.

Since the pilot symbols $\{S_{I_1}, S_{I_2}, ..., S_{I_p}, ...S_{I_P}\}$ and the data symbols $\{S_{J_1}, S_{J_2}, ..., S_{J_d}, ...S_{J_D}\}$ are not overlapped

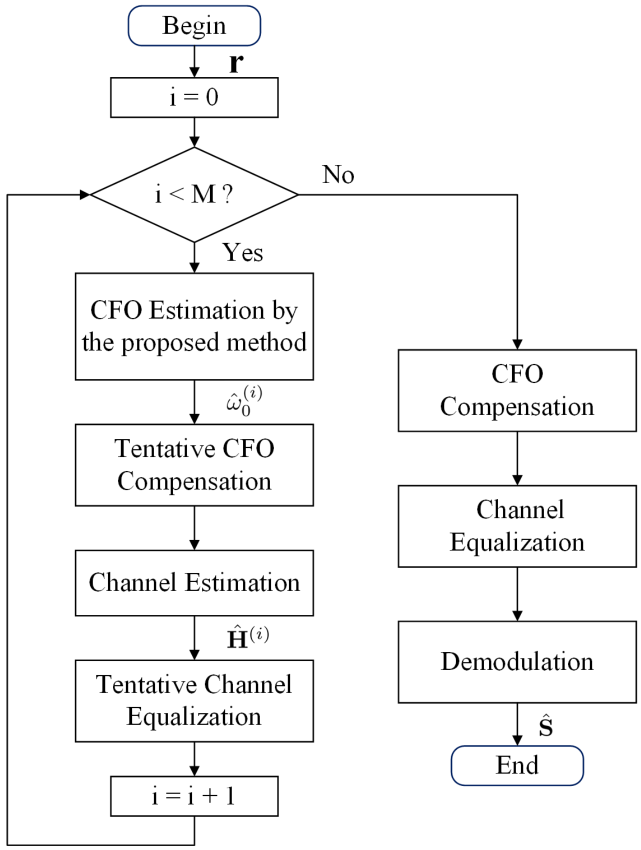

Fig. 1. The alternative CFO and channel estimation

in $\mathbf{S}$, the received signal related to the pilot symbols is conveniently extracted from $\mathbf{S}_d$. It results in

$$\underbrace{\begin{bmatrix} R_{I_1} \\ R_{I_2} \\ \vdots \\ R_{I_P} \end{bmatrix}}_{\mathbf{R}_h^P} = \underbrace{\begin{bmatrix} S_{I_1} & & & \\ & S_{I_2} & & \\ & & \ddots & \\ & & & S_{I_P} \end{bmatrix}}_{\mathbf{S}_d^P} \times \underbrace{\frac{1}{\sqrt{K}} \begin{bmatrix} 1 & e^{-j2\pi\frac{I_1}{K}} & \cdots & e^{-j2\pi\frac{I_1 L}{K}} \\ 1 & e^{-j2\pi\frac{I_2}{K}} & \cdots & e^{-j2\pi\frac{I_2 L}{K}} \\ \vdots & \vdots & \vdots & \vdots \\ 1 & e^{-j2\pi\frac{I_P}{K}} & \cdots & e^{-j2\pi\frac{I_P L}{K}} \end{bmatrix}}_{\tilde{\mathbf{F}}^P} \times \underbrace{\begin{bmatrix} h(0) \\ h(1) \\ \vdots \\ h(L) \end{bmatrix}}_{\mathbf{h}} + \underbrace{\begin{bmatrix} V_{h,I_1} \\ V_{h,I_2} \\ \vdots \\ V_{h,I_P} \end{bmatrix}}_{\mathbf{V}_h} \tag{9}$$

In its compact form, (9) becomes

$$\mathbf{R}_h^P = \mathbf{S}_d^P \tilde{\mathbf{F}}^P \mathbf{h} + \mathbf{V}_h \tag{10}$$

Based on (10), the least squares (LS) channel estimation is obtained as

$$\hat{\mathbf{h}} = (\mathbf{S}_d^P \tilde{\mathbf{F}}^P)^\dagger \mathbf{R}_h^P \tag{11}$$

There are $L+1$ unknown channel taps to be estimated and to obtain a reliable estimation, $P \geq L+1$ is required.

B. CFO Estimation

With the channel estimation in Section III-A as a prerequisite, the pilot-based CFO estimation can be performed. For a given CFO candidate ω, we perform the tentative CFO compensation as in (6).

$$\tilde{\mathbf{r}} = e^{j(\omega_0-\omega)\overline{L}} \mathbf{D}_K(\omega_0 - \omega)\mathbf{H}\mathbf{s} \tag{12}$$

With the estimated channel, the equalization can be performed. For the purpose of the CFO estimation, the equalization only needs to be performed for the pilot symbols. Specifically, for the pilot symbols with the index I_p, the equalized pilot symbols are

$$\hat{\mathbf{S}}^P(\omega) = \left(\hat{\mathbf{H}}_d^P\right)^\dagger \mathbf{R}^P(\omega) \tag{13}$$

where $\hat{\mathbf{S}}^P(\omega) = \{\hat{S}_{I_1}(\omega), \hat{S}_{I_2}(\omega), ..., \hat{S}_{I_P}(\omega)\}$ is the estimation of $\mathbf{S}^P = \{S_{I_1}, S_{I_2}, ..., S_{I_P}\}$ (the pilot part of $\mathbf{S}$) given the tentative CFO compensation with ω. $\hat{\mathbf{H}}_d^P = diag\{\tilde{\mathbf{F}}^P\hat{\mathbf{h}}\}$, $\mathbf{R}(\omega) = \mathbf{F}\tilde{\mathbf{r}}$, and $\mathbf{R}^P(\omega)$ consists of components of $\mathbf{R}(\omega)$ with the index I_p. $\hat{\mathbf{H}}_d^P$ consists of the channel frequency domain component corresponding to the pilot with index I_p. By (18), we can obtain the equalized pilot symbols $\hat{\mathbf{S}}^P(\omega)$ only by using $\mathbf{R}^P(\omega)$ instead of using the whole signal $\mathbf{R}(\omega)$. With the equalized pilot symbols $\{\hat{S}_{I_p}(\omega)\}$, we define the following CFO estimation metric:

$$\mathcal{C}(\omega) = \sum_{p=1}^{P} \left|\hat{S}_{I_p}(\omega) - S_{I_p}\right|^2 \tag{14}$$

If the CFO is correctly compensated, the square error given in (14) tends to be small. Hence, the estimate of ω_0 is obtained as:

$$\hat{\omega}_0 = \arg\min \mathcal{C}(\omega) \tag{15}$$

Note first that $\hat{\omega}_0 = \omega_0$ implies $e^{j(\omega_0-\omega)\overline{L}}\mathbf{D}_N(\omega_0-\omega) = \mathbf{I}_N$ and $\mathbf{r} = \mathbf{H}\mathbf{s} = \mathbf{h} * \mathbf{s}$ in (17). Take the Fourier transform of both sides of the $\mathbf{r} = \mathbf{h} * \mathbf{s}$, we have

$$\mathbf{R}(\omega) = \mathbf{H}_d \mathbf{S}(\omega) \tag{16}$$

Since the pilot symbols and the data symbols are nonoverlapping in $\mathbf{S}$, we have

$$\mathbf{R}^P(\omega) = \mathbf{H}_d^P \mathbf{S}^P(\omega) \tag{17}$$

and

$$\mathbf{S}^P(\omega) = \left(\mathbf{H}_d^P\right)^\dagger \mathbf{R}^P(\omega) \tag{18}$$

If the estimation of $\mathbf{H}_d$ is reliable, $\hat{\mathbf{H}}_d^P$ is close to $\mathbf{H}_d^P$. Hence, $\hat{\mathbf{S}}^P(\omega)$ is approximated to $\mathbf{S}^P(\omega)$ and $\mathcal{C}(\omega)$ become very small.

In order to find the closest CFO estimation $\hat{\omega}_0$ to ω_0, we use the one-dimensional search algorithm. The search procedure is divided into the following two steps. Firstly, we perform a coarse search over the candidate interval $[-\omega_m, \omega_m]$ (ω_m can be set to π because the period of CFO is 2π) with a coarse step size μ_c, leading to the coarse CFO estimation ω_c. Second, we narrow the candidate interval to a smaller range $(\omega_c - \mu_c, \omega_c + \mu_c)$, and we perform a fine search over it with a fine step size μ_f to produce a more accurate CFO ω_f estimation [2]. We can repeat the second step over a smaller candidate interval with a finer step size to obtain a more accurate ω_0 estimation.

However, through the simulation we find there are several local minimums of $\mathcal{C}(w)$ with similar values and only one of them refers to the correct CFO. After passing a multipath channel with white gaussian noise, the true minimum is hard to be distinguished among the local minimums. We find that the bit error ratio (BER) of pilot can lead to a certains interval which only contain the true minimum. Thus, we propose an improved method to achieve a more accurate CFO estimation. Firstly, we use the one-dimensional search algorithm to obtain an interval $[c, d]$ where the BER of the pilot is smaller than $\mathcal{E}$ ($\mathcal{E}$ can be to about 0.15 according to the experience). Then we use the one-dimensional search algorithm to obtain the ω_0 estimation among $[c, d]$.

Algorithm 1 One-Dimensional Search-Based CFO Estimation with the BER and the Square Error of the Pilot

Input:
The candidate interval $[-\omega_m, \omega_m]$;
The size-N_c CFO candidate array Ω, $\Omega(n_c) = -\omega_c + 2(n_c - 1)\omega_m/(N_c - 1), n_c = 1, ..., N_c$.
Initialization:
The empty metric set $\mathcal{B} = \{\}$;
The empty metric set $\mathcal{M} = \{\}$.
Interval narrowing:
FOR $n_c = 1$ TO N_c
1: Take the n_cth candidate CFO $\omega = \Omega(n_c)$;
2: Perform the CFO compensation $\bar{\mathbf{r}} = e^{j(\omega_0-\omega)\overline{L}}\mathbf{D}_K(\omega_0 - \omega)\,\mathbf{Hs}$ as in (17);
3: Perform the LS equalization on the pilot portions as in (18) to obtain $\hat{\mathbf{S}}^P(\omega)$;
4: If the BER of $\hat{\mathbf{S}}^P(\omega)$ is less than $\mathcal{E}$, push ω into $\mathcal{B}$;
END
Take the first and the last element of $\mathcal{B}$ as c and d respectively to obtain the new candidate interval $[c, d]$;
Fine estimation:
FOR $n_d = 1$ TO N_d
5: Take the n_dth candidate CFO $\omega = \Theta(n_d)$; $\Theta(n_d) = c + (n_d - 1)(d - c)/(N_d - 1), n_d = 1, ..., N_d$;
6: Perform the CFO compensation $\bar{\mathbf{r}} = e^{j(\omega_0-\omega)\overline{L}}\mathbf{D}_K(\omega_0 - \omega)\,\mathbf{Hs}$ as in (17);
7: Perform the LS equalization on the pilot tones as in (18) to obtain $\hat{\mathbf{S}}^P(\omega)$;
8: Compute the metric $\mathcal{C}(\omega)$ as in (19) and push it into $\mathcal{M}$;
END
Find the minimum of the N_c metrics in $\mathcal{M}$ in (20), and the corresponding CFO candidate is the final CFO estimation.
Output:
The estimated CFO $\hat{\omega}_0$.

IV. Simulation Results

In this section, we illustrate the estimated results through computer simulations. We use multipath channels and AWGN with zero-mean and variance σ_ω^2. The definition of signal-to-noise ratio (SNR) is SNR $= \delta^2/\sigma_\omega^2$ with normalized channel variance (i.e., $\sigma_h^2 = 1$), where δ^2 is the energy per symbol. The amplitudes of paths follow a Rayleigh distribution with the average power decreasing exponentially with the delay. The power difference between the first path and the last one is 20 dB.

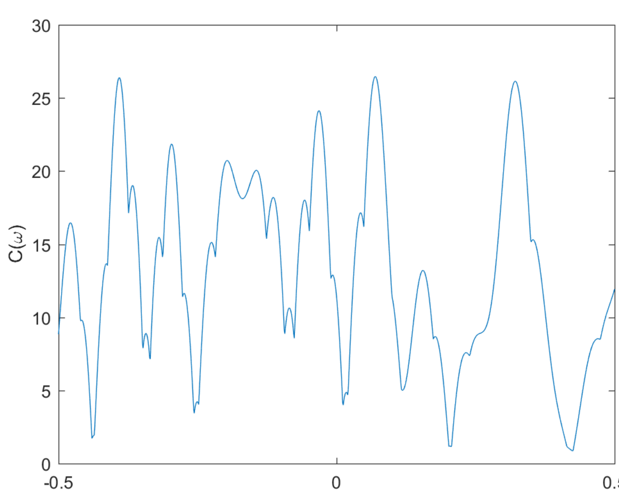

Fig. 2. The cost function $\mathcal{C}(\omega)$ in (19) vs. CFO with the true CFO being 0.224 and SNR = 1 dB

In Fig. 2 and Fig. 3, we set the CFO to be 0.224 and SNR to be 1. Fig. 2 shows the trend of $\mathcal{C}(\omega)$ with ω, from which we can find there are several local minimums. It is risky to directly use $\mathcal{C}(\omega)$ as in (20) to perform the estimation. Fig. 3 shows the trend of the pilot BER versus ω. It is obvious the pilot BER has a valley when ω is nearby 0.224. Because the BER curve is not smooth, we can not directly gain the accurate CFO estimation. But we could obtain a smaller interval which contains the CFO.

Fig. 4 shows the root mean squared error (RMSE) of the estimated CFO with different methods on OFDM. Fig. 5 shows BER of the demodulated signal with different methods on OFDM. The curves with the circular markers demonstrate the performance of method in [2], respectively. Furthermore, the curves with the square markers demonstrate the performance of our method. The CFOs estimated by our method have smaller RMSE. After CFO compensation and channel equalization, we can demodulate the signal. We achieve a lower BER, which means the recovered signals are more reliable with our method.

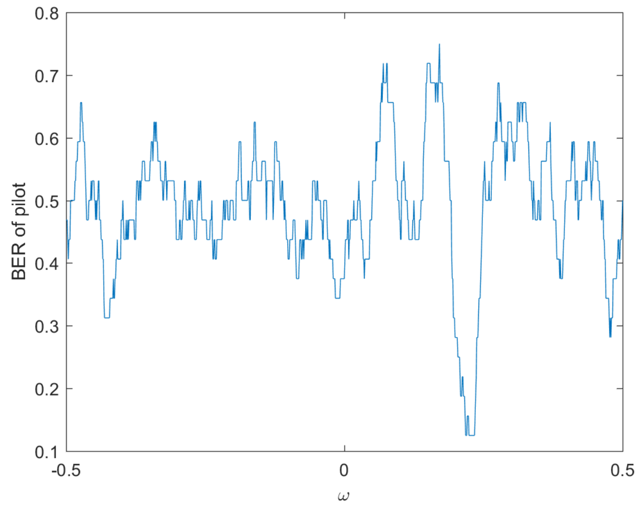

Fig. 3. BER of pilot symbols vs. CFO with the true CFO being 0.224 and SNR = 1 dB

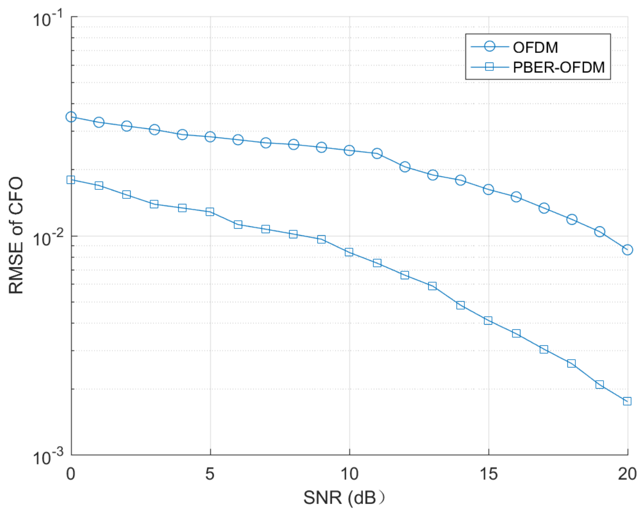

Fig. 4. RMSE of CFO vs. SNR under multipath channels

V. Conclusion

In this paper, we propose a new data-aided method to achieve CFO estimation for OFDM. We set the pilot to achieve both channal estimation and CFO estimation for OFDM. We show that the conventional approach of [3] might perform not so well under the severe effect of multipath and AWGN. Furthermore, We use the BER and the MSE of the pilot as the metrics to estimate the CFO by one-dimensional search. Ultimately, we achieve lower RMSE and BER on OFDM through the new method.

References

[1] X. Ma, C. Tepedelenlioğlu, G. B. Giannakis, and S. Barbarossa, "Non-data-aided carrier offset estimators for OFDM with null subcarriers: identifiability, algorithms, and performance," *IEEE Journal on Selected Areas in Communications*, vol. 19, no. 12, pp. 2504-2515, Dec. 2001.

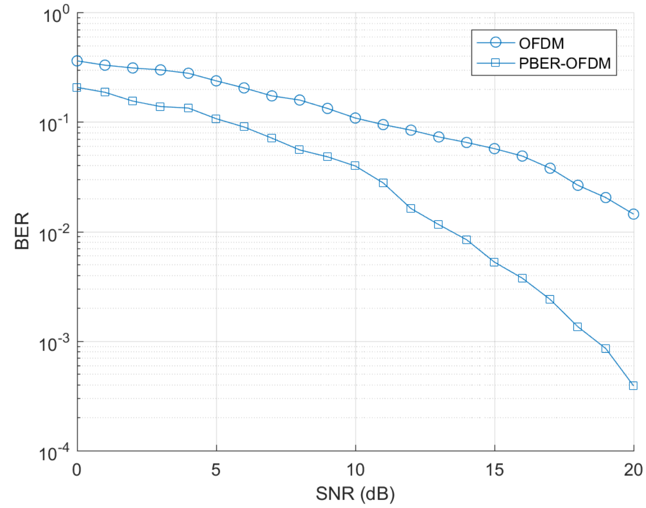

Fig. 5. BER vs. SNR under multipath channels

[2] J. Tao, "DFT-precoded MIMO OFDM underwater acoustic communications," *IEEE Journal of Oceanic Engineering*, vol. 43, no. 3, pp. 805-819, Jul. 2018. .

[3] Z. Wang and G. B. Giannakis, "Wireless multicarrier communications: where fourier meets shannon," *IEEE Signal Processing Magazine*, vol. 17, no. 3, pp. 29-48, May 2000.

[4] P. H. Moose, "A technique for orthogonal frequency division multiplexing frequency offset correction," *IEEE Trans. Communications*, vol. 42, pp. 2908-2914, Oct. 1994.

[5] G. Vazquez and J. Riba, "Non-data-aided digital synchronization," *IEEE Trans. Signal Processing*, vol. 2, ch. 9, pp. 357-402, 2000.

[6] U. Tureli, H. Liu, and M. D. Zoltowski, "OFDM blind carrier offset estimation: ESPRIT," *IEEE Trans. Communications*, vol. 48, pp. 1459-1461, Sept. 2000.

[7] T. M. Schmidl and D. C. Cox, "Robust frequency and timing synchronization for OFDM," *IEEE Trans. Communications*, vol. 45, no. 12, pp. 1613-1621, Dec. 1997.

[8] S. Barbarossa, M. Pompili, and G. B. Giannakis, "Time and frequency synchronization of orthogonal frequency division multiple access systems," *IEEE International Conference on Communications*, vol. 6, pp. 1674-1678, June 11-15, 2001.

[9] J. van de Beek, M. Sandell, and P. O. Brjesson, "ML estimation of time and frequency offset in OFDM systems," *IEEE Trans. Signal Processing*, vol. 45, pp. 1800-1805, July 1997.

[10] H. Bolcskei, "Blind high-resolution uplink synchronization of OFDM-based multiple access schemes," *IEEE Workshop Signal Processing Advances in Wireless Communications*, Annapolis, MD, 1999, pp. 166-169.

[11] H. Liu and U. Tureli, "A high efficiency carrier estimator for OFDM communications," *IEEE International Conference on Communications*, vol. 2, pp. 104-106, Apr. 1998.

[12] M. Luise and R. Reggiannini, "Carrier frequency offset acquisition and tracking for OFDM systems," *IEEE Trans. Communications*, vol. 44, pp. 1590-1598, Nov. 1996.

[13] X. Ma, G. B. Giannakis, and S. Barbarossa, "Non-data-aided frequency offset and channel estimation in OFDM and related block transmissions," *IEEE International Conference on Communications*, vol. 6, pp. 1866-1870, Jun. 2001.

[14] T. Pollet, M. Van Bladel, and M. Moenaclaey, "BER sensitivity of OFDM systems to carrier frequency offset and Wiener phase noise," *IEEE Trans. Communications*, vol. 43, pp. 191-192, Apr. 1995.

[15] J. M. Wen, Y. Zhang, and M. Xiao, "The Talbot effect: recent advances in classical optics, nonlinear optics, and quantum optics," *Advances in Optics and Photonics*, vol. 5, no. 1, pp. 83-130, Mar. 2013.